

INTRIGUING RELATIONS BETWEEN THE LECs OF WILSON χ -PT AND SPECTRA OF THE WILSON DIRAC OPERATOR*

MARIO KIEBURG^a, JACOBUS J.M. VERBAARSCHOT^b
SAVVAS ZAFEIROPOULOS^{b,c}

^aFakultät für Physik, Universität Bielefeld
Postfach 100131, 33501 Bielefeld, Germany

^bDepartment of Physics and Astronomy, Stony Brook University
NY 11794-3800, USA

^cLaboratoire de Physique Corpusculaire, Université Blaise Pascal, CNRS/IN2P3
63177 Aubière Cedex, France

(Received June 17, 2014)

We discuss the behavior of the spectral densities of the non-Hermitian Wilson Dirac operator. Moreover, we derive compact relations between the leading order LECs of Wilson χ -PT and observables that can be measured by a lattice simulation. These relations can be used to determine the LECs from lattice simulations.

DOI:10.5506/APhysPolBSupp.7.625

PACS numbers: 12.38.Gc, 05.50.+q, 02.10.Yn, 11.15.Ha

1. Introduction

Wilson fermions are widely used in high precision lattice studies which can confront experiments as well as in theoretical studies beyond the Standard Model. The current supercomputers and the algorithmical developments have allowed for simulations in the deep chiral regime. Since high accuracy is sought after in these studies, it is expedient to have the lattice discretization errors under tight analytical control. There has been a plethora of approaches addressing this issue. The determination of the Low Energy Constants (LECs) of Wilson chiral perturbation theory [1] has been attempted analytically [2–8] as well as numerically [9–15] in order to shed new light on the unphysical phases that one encounters in the chiral limit at finite lattice spacing. Discretization artifacts have also been considered for QCD-like theories [16] and they could potentially facilitate technicolor studies.

* Presented by S. Zafeiropoulos at “Excited QCD 2014”, Bjelašnica Mountain, Sarajevo, Bosnia and Herzegovina, February 2–8, 2014.

In this study, we incorporate the effect of the three LECs to the leading order. Our starting point is the Wilson random matrix theory (RMT) for the non-Hermitian Wilson Dirac operator originally introduced in [2]. We refer the reader to [17] for a review of the recent developments of Wilson RMT as well as to [5] for the relevant mathematical developments. In this paper, we summarize the main results of Ref. [8].

2. Wilson χ -PT in the ϵ -regime

The drastic step of Wilson to include the lattice discretization of the Laplacian in order to get rid of the doublers is to give up chiral symmetry. This has profound consequences for the low energy effective theory of QCD with the N_f flavor partition function given by

$$Z_{N_f}^\nu(m) = \int_{\mathbf{U}(N_f)} d\mu(U) \exp \left[\frac{\Sigma V}{2} \text{tr} m (U + U^{-1}) - a^2 V W_6 \text{tr}^2 (U + U^{-1}) \right] \\ \times \exp \left[-a^2 V W_7 \text{tr}^2 (U - U^{-1}) - a^2 V W_8 \text{tr} (U^2 + U^{-2}) \right] \det^\nu U, \quad (1)$$

where m is the quark mass, a is the lattice spacing, Σ is the chiral condensate and V is the space time volume. As is always the case in χ -PT, one needs to adopt a power counting scheme and, in our case, it is the ϵ -counting since it makes direct contact with the Random Matrix Theory [18–20]. In this regime, the combinations mV as well as a^2V are fixed. Note that the p -regime [1, 4] shares the same potential to lowest order.

3. Extraction of Σ and $W_{6/7/8}$

At finite lattice spacing, the Wilson Dirac operator is no longer Hermitian. It still retains the very important property of γ_5 -Hermiticity, $D_W^\dagger = \gamma_5 D_W \gamma_5$, which has important consequences for the eigenvalues and eigenvectors. In particular, the eigenvalues of the Wilson Dirac operator come in complex conjugate pairs or are real, and only the eigenvectors corresponding to real eigenvalues have non-vanishing chirality. Generically, the Dirac operator, at fixed index ν will have at least ν real eigenvalues. The additional eigenvalues originate from the collision of a complex conjugate pair which may enter the real axis. Because of this, we can define three different eigenvalue densities, the density of the complex eigenvalues, ρ_c , the total density of the real modes, $\rho_{\text{real}} = \rho_{\text{right}} + \rho_{\text{left}}$, and the difference, $\rho_\chi^\nu = \rho_{\text{right}} - \rho_{\text{left}}$ of the density of the right-handed real modes ($\langle \psi | \gamma_5 | \psi \rangle > 0$) and the density of the left-handed real modes ($\langle \psi | \gamma_5 | \psi \rangle < 0$). The difference ρ_χ^ν is equal to

the distribution of the chirality over the real eigenvalues [3]

$$\rho_\chi^\nu(\hat{\lambda}) \equiv \sum_{\hat{\lambda}_k \in \mathbb{R}} \delta(\hat{\lambda} - \hat{\lambda}_k) \text{sign}\langle k | \gamma_5 | k \rangle \quad (2)$$

which can be expressed in terms of the imaginary part of the resolvent

$$\rho_\chi^\nu(\hat{\lambda}) = \lim_{V \rightarrow \infty} \frac{1}{\pi} \text{Im} \left[G^\nu(\hat{\lambda}) \equiv \left\langle \text{tr} \frac{1}{V \Sigma D_W + \hat{\lambda} \mathbf{1} - i\epsilon \gamma_5} \right\rangle \right]. \quad (3)$$

This distribution obeys the normalization condition $\int \rho_\chi(\hat{x}) d\hat{x} = \nu$. The variance of this distribution at fixed index ν , close to the continuum limit, is determined by the LECs, *i.e.*

$$\frac{\langle x^2 \rangle_{\rho_\chi}}{\Delta^2} \stackrel{\hat{a} \ll 1}{\approx} \frac{8}{\pi^2} V a^2 (\nu W_8 - W_6 - W_7), \quad \nu > 0. \quad (4)$$

Plotting this quantity *versus* the index ν of the Dirac operator yields both W_8 and the sum $W_6 + W_7$.

The average number of additional real modes,

$$N_{\text{add}} = \int_{-\infty}^{\infty} \rho_{\text{add}}(\hat{x}) d\hat{x}, \quad (5)$$

is also a useful quantity for measuring the strength of the lattice artifacts. Close to the continuum, the average number of additional real modes scales as $\hat{a}^{2\nu+2}$, while it scales linearly with \hat{a} and becomes independent of ν in the limit of large lattice spacing, see Fig. 1. Thus, at small lattice spacing almost all additional real modes come from the sector with index $\nu = 0$ and are given by

$$N_{\text{add}}^{\nu=0} \stackrel{\hat{a} \ll 1}{\approx} 2V a^2 (W_8 - 2W_7). \quad (6)$$

At large volumes, where most configurations have $\nu \neq 0$, the additional real modes are suppressed. Therefore, “exceptional configurations”, *i.e.* configurations where the eigenvalue λ of the Dirac operator is almost equal to $-m$ potentially jeopardizing the inversion of the Dirac operator, are not too much of a problem.

In Fig. 2, we show the projected density of complex eigenvalues,

$$\rho_{\text{cp}}(\hat{y}) = \int_{-\infty}^{\infty} \rho_c(\hat{x} + i\hat{y}) d\hat{x}, \quad (7)$$

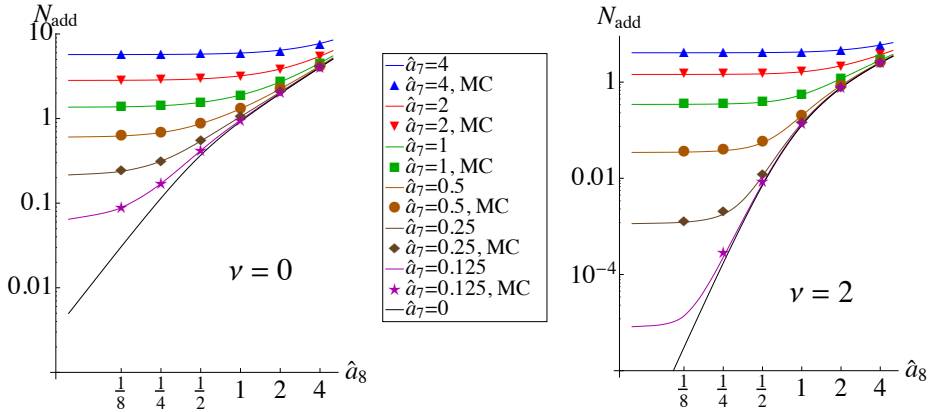


Fig. 1. Log–log plots of the average number of additional real modes *versus* \hat{a}_8 for $\nu = 0$ (left plot) and $\nu = 2$ (right plot). The analytical results (solid curves) are compared to Monte Carlo simulations of RMT (symbols). A non-zero value of \hat{a}_7 yields a saturation at small \hat{a}_8 . The difference in the order of magnitude between the cases of $\nu = 0$ as well as $\nu \neq 0$ is also noteworthy.

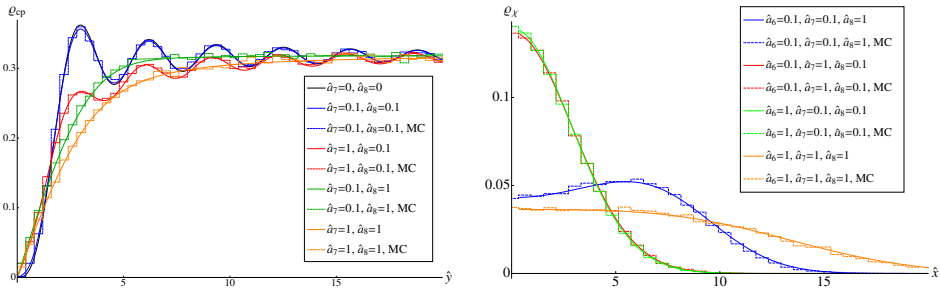


Fig. 2. Analytical results for the projected level density of complex eigenvalues onto the imaginary axis, ρ_{cp} , (left) and for the distribution of the chirality over the real modes, ρ_χ , (right) *versus* MC simulations of Wilson RMT for $\nu = 1$. The black curve in the left plot is the result in the continuum and agrees very well with ρ_{cp} for small values of the lattice spacing.

for several values of W_7 and W_8 . For small lattice spacing, this distribution is close to the continuum result making this a good quantity to extract the chiral condensate via the Banks–Casher relation,

$$\Delta \hat{a} \leq 1 \frac{\pi}{\Sigma V}, \tag{8}$$

where Δ is the average level spacing of the imaginary part of the eigenvalues close to the origin. Moreover, for small values of the lattice spacing, the

section of ρ_c parallel to the real axis is a Gaussian of width given by

$$\frac{\sigma^2}{\Delta^2} \stackrel{\hat{a} \ll 1}{\cong} \frac{4}{\pi^2} a^2 V(W_8 - 2W_6), \quad (9)$$

serving as a good quantity to extract the combination $W_8 - W_6$.

4. Conclusions

We summarized analytical results for the eigenvalue density of the non-Hermitian Wilson Dirac operator D_W in the quenched limit (see [5, 6, 8]). In a forthcoming publication, we plan to generalize these results to include dynamical fermions. These analytical results yield simple relations between the LECs, Σ and $W_{6/7/8}$, and some observables measurable in lattice simulations such as the average level spacing of the projected eigenvalues onto the imaginary axis and the average number of additional real modes, *cf.* Eqs. (4), (6), (8), and (9). These relations were obtained for small lattice spacing $|a^2 V W_{6/7/8}| \leq 0.1$, which is in a domain that corresponds to realistic lattice parameters. In particular, simulations with a clover improved action [14] have shown that this regime is easily accessible. Employing the parameters of [14], the LECs can be measured with an error estimate between 1%–10%, which can certainly be improved. Moreover, our analysis shows that a non-zero amount of additional real modes automatically requires either a non-zero W_7 or a non-vanishing W_8 . However, exactly this number is strongly suppressed for configurations corresponding to non-trivial topological configurations. Most of the additional real modes result from configurations with the index $\nu = 0$. This shows that configurations where the massive Dirac operator exhibits zero modes are quite rare and will not have much of an impact in realistic simulations.

M.K. acknowledges financial support by the Alexander-von-Humboldt Foundation. J.V. and S.Z. acknowledge support by the U.S. DOE Grant No. DE-FG-88ER40388. We thank Gernot Akemann, Poul Damgaard, Urs Heller and Kim Splittorff for fruitful discussions.

REFERENCES

- [1] S.R. Sharpe, R.L. Singleton, Jr., *Phys. Rev.* **D58**, 074501 (1998).
- [2] P.H. Damgaard, K. Splittorff, J.J.M. Verbaarschot, *Phys. Rev. Lett.* **105**, 162002 (2010).
- [3] G. Akemann, P.H. Damgaard, K. Splittorff, J. Verbaarschot, *PoS LATTICE2010*, 079 (2010); *LATTICE2010*, 092 (2010); *Phys. Rev.* **D83**, 085014 (2011).

- [4] S. Necco, A. Shindler, *J. High Energy Phys.* **1104**, 031 (2011).
- [5] M. Kieburg, *J. Phys. A* **45**, 095205 (2012); **45**, 205203 (2012) some minor amendments where done in a newer version at [arXiv:1202.1768v3](https://arxiv.org/abs/1202.1768v3) [math-ph].
- [6] M. Kieburg, J.J.M. Verbaarschot, S. Zafeiropoulos, *PoS LATTICE2011*, 312 (2011); *Phys. Rev. Lett.* **108**, 022001 (2012).
- [7] M. Kieburg, K. Splittorff, J.J.M. Verbaarschot, *Phys. Rev.* **D85**, 094011 (2012).
- [8] M. Kieburg, J.J.M. Verbaarschot, S. Zafeiropoulos, *Phys. Rev.* **D88**, 094502 (2013).
- [9] R. Baron *et al.* [ETM Collaboration], *J. High Energy Phys.* **1008**, 097 (2010) [[arXiv:0911.5061](https://arxiv.org/abs/0911.5061)] [hep-lat].
- [10] C. Michael *et al.* [ETM Collaboration], *PoS LAT2007*, 122 (2007).
- [11] S. Aoki, O. Bär, *Eur. Phys. J.* **A31**, 781 (2007).
- [12] A. Deuzeman, U. Wenger, J. Wuilloud, *J. High Energy Phys.* **1112**, 109 (2011); *PoS LATTICE2011*, 241 (2011).
- [13] F. Bernardoni, J. Bulava, R. Sommer, *PoS LATTICE2011*, 095 (2011).
- [14] P.H. Damgaard, U.M. Heller, K. Splittorff, *Phys. Rev.* **D85**, 014505 (2012); **D86**, 094502 (2012).
- [15] G. Herdoiza *et al.*, *J. High Energy Phys.* **1305**, 038 (2013).
- [16] M. Kieburg, J.J.M. Verbaarschot, S. Zafeiropoulos, *PoS LATTICE2012*, 209 (2012).
- [17] K. Splittorff, *PoS LATTICE2012*, 018 (2012).
- [18] E.V. Shuryak, J.J.M. Verbaarschot, *Nucl. Phys.* **A560**, 306 (1993).
- [19] J.J.M. Verbaarschot, *Phys. Rev. Lett.* **72**, 2531 (1994).
- [20] J.C. Osborn, D. Toublan, J.J.M. Verbaarschot, *Nucl. Phys.* **B540**, 317 (1999).